Molecular Structures of Phthalocyaninatozinc and Hexadecafluorophthalocyaninatozinc Studied by Gas-Phase Electron Diffraction and Quantum Chemical Calculations

Tatyana Strenalyuk, Svein Samdal,* and Hans Vidar Volden

Department of Chemistry, Centre for Theoretical and Computational Chemistry, University of Oslo, P.O. Box 1033 Blindern, NO-0315 Oslo, Norway

The molecular structures of phthalocyaninatozinc (HPc-Zn) and hexadecafluorophthalocyaninatozinc (FPc-Zn) are determined using the gas electron diffraction (GED) method and high-level density functional theory (DFT) quantum chemical calculations. Calculations at the B3LYP/6-311++G** level indicate that the equilibrium structures of HPc-Zn and FPc-Zn have D_{4h} symmetry and yield structural parameters in good agreement with those obtained by GED at 480 and 523 °C respectively. The calculated force fields indicate that both molecules are flexible. Normal coordinate calculations on HPc-Zn yield five vibrational frequencies (one degenerate) in the range 22–100 cm^{-1}, and ten vibrational frequencies ranging from 13 to 100 cm^{-1} (three degenerate) for FPc-Zn. The high-level force field calculations confirm most of the previous vibrational assignments, and some new ones are suggested. The out-of-plane vibration of the Zn atom in HPc-Zn was studied in detail optimizing models in which the distance from the Zn atom to the two symmetry equivalent diagonally opposed *N* atoms (*h*) was fixed. The calculations indicate that the vibrationally activated vertically displacement of the Zn atom is accompanied by distortion of the ligand from D_{4h} to C_{2v} symmetry. The average height, *h*, at the temperature of the GED experiment was calculated to be 14.5 pm. Small structural changes indicate that a full F substitution on the benzo-subunits do not significantly alter the geometry, however there are indications that the benzo-subunits may shrink slightly with perfluorination.

Introduction

Metal phthalocyanines (MPcs) represent a class of organic materials that attracts great attention in several different fields of science and industry. Their high thermal and chemical stability have made them suitable for many technological applications such as dyes, pigments, semiconductors, energy conversion in photovoltaic and solar cells, photosensitizers, electrophotography, molecular electronics, gas sensors, electrochromism in display devices, liquid crystals, Langmuir–Blodgett films, nonlinear optics, electrocatalytic reagents, and photodynamic therapy. Due to the similarity in structure to biologically important molecules such as chlorophyll and hemoglobin they have caught special interest. There are several excellent books about MPcs where the above-mentioned properties and applications are discussed.[1–6]

SciFinder gives about 39 000 hits on phthalocyanines. In spite of this huge amount of information about Pcs, there is almost nothing known about their molecular structures in the gas phase. MPcs are thermally stable compounds, and sublimation is used both for purification and for creation of thin films for different purposes. It should therefore be possible to get useful information about the molecular structures of these compounds in the gas phase using the gas electron diffraction (GED) method. GED is the only method suitable to determine the molecular geometry for such large molecules in the gas phase. The only GED investigations so far have been carried out by Fink and his co-workers who have studied HPc-Zn[7] in 1993, HPc-Sn and HPc-Mg and reinvestigated HPc-Zn[8] in 1999, and HPc-Cu and HPc-Ni[9] in 2000. The reasons MPcs have not been more extensively studied by the GED method might be related first to the lack of equipment to heat the effusion cell to a sufficiently high temperature to evaporate the compound and second to the fact that most GED laboratories have used photographic plates to record data that might make it more difficult to obtain good data than using image plates. Fink and his co-workers avoided this problem by using an electron counting device,[7] but this is a time-consuming process and the collection of a data set may take as much as 24 h and the observed scattering range is usually small compared to conventional GED investigations. The data range for HPc-Zn was up to $s = 145$ pm^{-1}, which made the precision and accuracy of the obtained structural parameters less reliable than usually obtained by the GED method.

Since 2000 we have been using the image plate (IP) technology to record the GED data. The IPs are more sensitive, have higher resolution, have a more linear response that makes blackness correction unnecessary, and have a much larger dynamic range than photographic plates. Diffraction data from gaseous benzene, which is used for calibration of the electron wavelength have shown that the reproducibility and accuracy obtained by using IPs are better than for photographic plates,[10] which should make the IPs particular suitable for recording data at high temperatures. We have recently successfully investigated F-SubPc with molecular formula $C_{24}BClF_{12}N_6$, systematic name chloro[1,2,3,4,8,9,10,11,15,16,17,18-dodecafluoro-7,12:14,19-diimino-21,5-nitrilo-5*H*-tribenzo[*c*,*h*,*m*]^{1,6,11} triazacyclopentadecinato(2–)κN22,κN23,κN24]boron(III) and trivial name chlorododecafluorosubphthalocyanatoboron(III) by GED,[11] and a natural extension would be to determine the molecular geometry of MPcs in the gas phase.

There is a rather limited amount of high-level quantum chemical calculations available on MPcs. Mostly semiempirical

* Corresponding author. E-mail: svein.samdal@kjemi.uio.no. Phone: 47 2285 5458. Fax +47 2285 5441.

and molecular mechanics methods have been used, obviously because of the molecular size and time-consuming calculations. For HPc-Zn there are conflicting predictions of the equilibrium geometry, one B3LYP/6-31G* calculation predicts a planar D_{4h} geometry,[8] another B3LYP/6-31G* calculation predicts a non-planar C_{4v} geometry[12] where the Zn atom is 7.5 pm above the *Pc* plane. The first GED investigation[7] of HPc-Zn concluded with a nonplanar C_{4v} geometry where the Zn atom is 34(13) pm above the *Pc* plane, whereas the reinvestigation concluded with a planar D_{4h} geometry[8] with the Zn atom in the symmetry plane. Moreover, there is a substantial disagreement between some of the C−C bond distances determined by GED[7,8] for HPc-Zn on one hand and by the quantum chemical calculations or the X-ray diffraction structure[13] on the other.

There are also a limited number of force field calculations and vibrational assignments for MPcs. B3LYP/6-31G** calculations have been used to calculate IR and Raman intensities for HPc-Zn[12,14] and to assign the fundamental frequencies. However, larger basis sets including diffuse and polarization functions are probably needed to give good predictions of the IR intensities[15,16] or Raman intensities.[17,18] MPcs have been considered as rather rigid molecules, but force field calculations predict several low-frequency modes, and this might have serious consequences for a GED analysis. The calculated root-mean-square amplitudes of vibration (*u*-values) from the molecular force field are nowadays always used in GED investigations to get more reliable *u*-values than those transferred from smaller fragments of the molecules. The previous investigations on HPc-Zn have neither used calculated *u*-values from forces field calculations nor explored the affect of the shrinkage correction, which might affect the determination of the molecular geometry.

We present here our results from GED and high-level quantum chemical studies on the structures of the molecules HPc-Zn with molecular formula $C_{32}H_{16}N_8Zn$, systematic name [29*H*,31*H*-phthalocyaninato(2−)-κN29,κN3O,κN31,κN32]zinc-(II) and trivial name phthalocyaninatozinc, and FPc-Zn with molecular formula $C_{32}F_{16}N_8Zn$, systematic name [1,2,3,4,8,9,-10,11,15,16,17,18,22,23,24,25-hexadecafluoro-29*H*,31*H*-phtha-locyaninato(2−)-κN29,κN3O,κN31,κN32]zinc(II) and trivial name hexadecafluorophthalocyaninatozinc. The latter has been included because it has been claimed that the properties of MPcs are little influenced by a peripheral substitution.

Experimental Section

Both compounds, HPc-Zn and FPc-Zn, were obtained from Aldrich and used without further purification.

The gas electron diffraction (GED) data were recorded on the Balzers KD-G2 unit[19] at the University of Oslo with use of an accelerating voltage of about 42 kV and a high-temperature stainless steel inlet system.[20,21] Experimental data were recorded on FujiFilm BAS-III image plates, and they were scanned with a FujiFilm BAS-1800II scanner. The image plate has a rectangular shape of approximately 13×18 cm². The data are collected and averaged over sectors along the positive and negative *y*-axis (short axis) and *x*-axis (long axis). More details about handling[10] of the experimental data and their processing[22] are given elsewhere.

The measured temperature represents the oven temperature and is measured with a Cu/constantan thermocouple. The thermocouple is placed outside the metal oven, and the dimension of the oven is approximately $7 \times 2 \times 2$ cm³. The nozzle opening is connected to the oven and is approximately 4 cm from the thermocouple. The measured oven temperature is assumed to be the temperature of the gas sample.
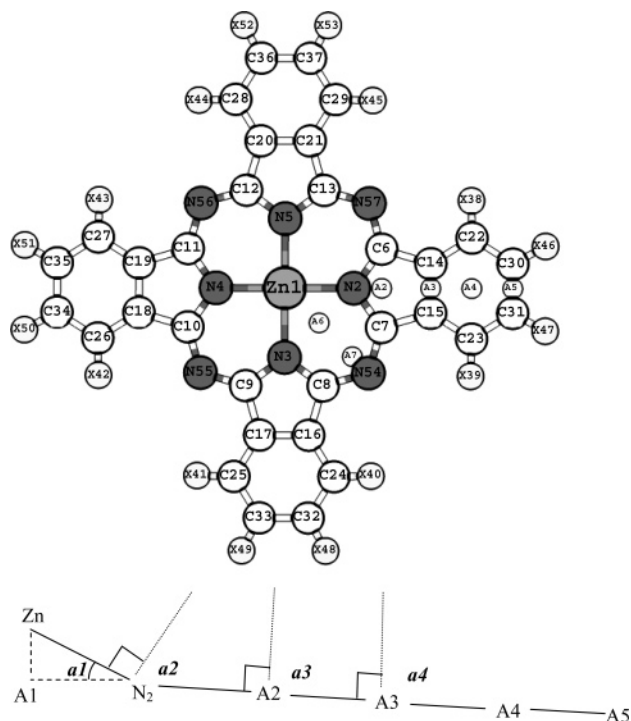

Figure 1. Molecular numbering of XPc-Zn (X = H or F) together with some auxiliary points. The figure below shows possible bending of isoindole unit under C_{4v} symmetry.

The modification and scattering functions were computed from tabulated atomic scattering factors[23] for the proper wavelength and *s* values. The experimental backgrounds were computed with the program KCED12,[24] where the coefficients of a chosen degree of a polynomial function are determined by the least-squares method by minimizing the differences between the experimental intensity and the currently best geometrical model on the modified form. A background is subtracted from data obtained for each individual sector. An average experimental intensity curve is obtained along the *y*- and *x*-axis, respectively giving two average experimental intensity curves for each camera distance as shown in Figure 2 and 3. The experimental conditions are summarized in Table 1.

Quantum Chemical Calculations. The quantum chemical calculations were performed with the GAUSSIAN03 program package[25] running on the HP "superdome" facilities in Oslo. The functional used for the calculations was the Becke three-parameter (B3LYP) hybrid functional,[26,27] which has been widely used in theoretical studies of pyrrole macrocycles.[28−38] Our previous experience with quantum chemical calculations on F-SubPc with different methods and basis sets confirms that DFT gives good agreement with the experimental results.[11] The basis sets we have used are 6-31G*,[39] 6-31++G**, 6-311++G**,[40,41] cc-pVTZ(H,C,N,F),[42] and cc-pVTZ-NR(Zn).[43] To our knowledge, the present calculations represent the highest level performed so far on HPc-Zn and FPc-Zn. The molecular geometry was optimized by assuming different symmetries. The numbering of the atoms is shown in Figure 1. The most important structural parameters are given in Table 2. The Cartesian coordinates from the B3LYP/cc-pVTZ calculations for HPc-Zn and FPc-Zn are given as Supporting Information (Table S1 and S2).

Molecular force field calculations were carried out for all basis sets except for DFT/cc-pVTZ, which requires too much computer time, to ensure that the stationary points represent a minimum. The *u*-values and shrinkage correction values,
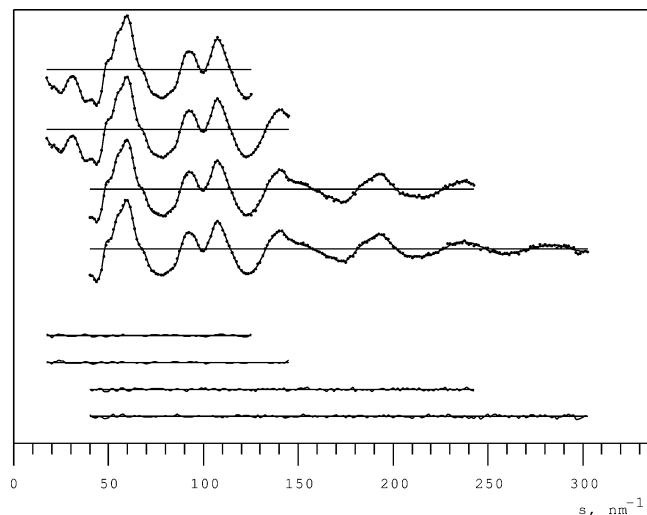
Molecular Structures of Phthalocyaninatozincs

J. Phys. Chem. A, Vol. 111, No. 47, 2007 **12013**

Figure 2. Average molecular intensity curves for HPc-Zn. The first two curves are the average from eight sectors from the long camera distance along the y- and *x*-axis, respectively. The two next curves are the corresponding average curves from eight sectors from the middle camera distance. Dots are experimental points and a full line is a theoretical curve. The four curves below are difference curves.
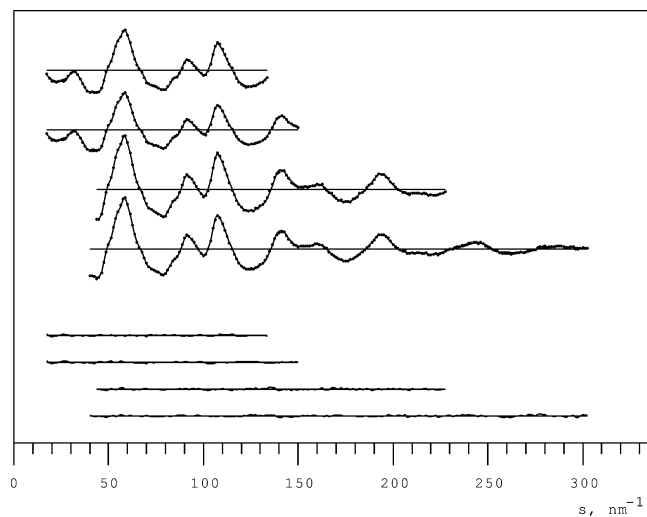

Figure 3. Average molecular intensity curves for FPc-Zn. The first two curves are the average from eight sectors from the long camera distance along the y- and *x*-axis, respectively. The next two curves are the corresponding average curves from eight sectors from the middle camera distance. Dots are experimental points, and a full line is the theoretical curve. The four curves below are difference curves.

k-values, used for shrinkage correction in the GED analysis were calculated from the B3LYP/6-311++G** force field. The proposed assignment of the IR and Raman spectra have mainly been based on calculated IR and Raman intensities from the quantum chemical calculations.[12,14] Because the reliability of the IR and Raman intensities are improved by introduction of diffuse and polarization functions,[15−18] and because there is little information about how these intensities change with inclusion of such functions, we have included these intensities together with the calculated frequencies as Supporting Information (Table S3).

Structure Analysis. The electron diffraction technique is described elsewhere.[44,45] A brief description that should be particularly relevant for this investigation to understand the assumptions made, to understand the precision and accuracy obtained for the structural parameters, and to judge the experimental results is given in the study of F-SubPc.[11]

HPc-Zn and FPc-Zn have similar molecular structures with a symmetrical *Pc* macrocycle composed of four isoindole units and a central cavity accommodating a Zn atom. In the case of FPc-Zn all H atoms are replaced with F atoms. Owing to the structural similarity of these two molecules, structural analysis was processed in the same manner for both molecules. The molecular symmetry was assumed to be C_{4v}, which can easily be constrained to D_{4h} during the analysis. The numbering of the atoms and auxiliary points is shown on Figure 1.

The molecular geometry of HPc-Zn and FPc-Zn can be modeled by rotating the isoindole fragment (N2, C6, C7, C14, C15, C22, C23, C30, C31, X38, X39, X46, X47, where X = H or F) 90.0°, 180°, and 270° about the 4-fold symmetry axis. The following set of independent parameters was composed to describe the molecular geometry: bond lengths Zn1−N2, N2−C6, C6−C14, C14−C15, C14−C22, C22−C30, C30−C31, C22−X38 C30−X46, bond angles C6−N2−C7, C15−C14−C22, C14−C22-X38, C22−C30-X46; dihedral angles C15−C14−C22−X38, C14−C22−C30−X46, which are all assumed 180.0°.

In addition five more parameters shown in Figure 1 were used to test whether average molecular structure possessed C_{4v} symmetry or D_{4h} symmetry. These parameters are the angle Zn1−N2−A1 (*a1*), where A1 is an auxiliary point used to define the position of the Zn atom out of central cavity, the angle Zn1−N2−A2 (*a2*) that defines the pyramidality of the N2 atom, the angle N2−A2−A3 (*a3*) defining the planarity of the pyrrole ring, and the angle A2−A3−A4 (*a4*) that defines the folding of the isoindole unit about the C14−C15 bond, and finally the angle N54−A6−A7 which defines the conformation of the ring consisting of the atoms Zn1, N2, C7, N54, C8, N3. If N54 is above the plane through the atoms N2, C7, C8, N3, the ring has a boat conformation, and if N54 is below, it has a chair conformation.

It is difficult to determine accurate structural parameters by the GED method where H atoms are involved due to the low scattering power of the H atoms. It is also difficult to determine accurate differences between bond lengths if the bond type and bond lengths are similar. This is the reason for introducing the following constraints: $r(C14C22) = r(C14C15) + \Delta1$, $r(C22C30) = r(C14C15) + \Delta2$, $r(C30C31) = r(C14C15) + \Delta3$, $r(C30X46) = r(C22X38) + \Delta4$ and $r(N54C7) = r(N2C6) + \Delta5$. The differences $\Delta1−5$ for HPc-Zn were taken from the quantum chemical calculation at the B3LYP/6-311++G** level, and were −1.57, −1.72, −0.37, +0.10, and −4.21 pm, respectively. The differences $\Delta1−5$ for FPc-Zn were taken from the B3LYP/6-311++G** calculation and were -2.51, −2.38, −1.56, +0.15, and −4.33 pm, respectively.

With these parameters and restrictions the molecular geometry can adapt D_{4h} symmetry, C_{4v} symmetry with a planar *Pc* and the Zn atom above the *Pc* plane, or C_{4v} symmetry with a concave shape of macrocycle and a square pyramidal coordination of a central Zn atom.

The shrinkage effect can be corrected for by using either a rectilinear[46,47] or a curvilinear[48,49] treatment of the vibrating atoms. The program SHRINK[48,49] was used to calculate these shrinkage correction terms k_{h0} (rectilinear) and k_{h1} (curvilinear), *u*-values, and the $r_a − r_e$ differences from the B3LYP/6-311++G** molecular force field. The curvilinear approach is generally considered to be the more realistic. Both the rectilinear and curvilinear approaches were tested, and the final results are given in Table 3 for HPc-Zn and in Table 4 for FPc-Zn. Comparison between experimental and theoretical results is given in Table 5 and 6. The *u*-values were refined in groups.

TABLE 1: Experimental Conditions for the GED Investigation of HPc-Zn and FPc-Zn

	HPc-Zn		FPc-Zn	
nozzle temp/ °C	480	480	523	523
nozzle-to-plate distance/mm	498.73	248.75	498.67	248.87
number of plates	4	4	4	4
s-range:				
x-direction/nm^{-1}	17.50−145.00	40.00−302.50	17.50−150.00	40.00−302.50
y-direction/nm^{-1}	17.50−125.00	40.00−242.50	17.50−133.75	43.75−227.50
Δs/nm^{-1}	1.25	1.25	1.25	1.25
accelerating voltage/kV	42	42	42	42
electron wave length/pm	5.82	5.82	5.82	5.82
degree of polynomial[a]	8	10	9	12

[a] Degree of polynomial used in the background subtraction

TABLE 2: Calculated Molecular Geometry[a] (D_{4h}) Using B3LYP for HPc-Zn and FPc-Zn

	HPc-Zn				FPc-Zn		
	6-31G*	6-31++G**	6-311++G**	cc-pVTZ	6-31G*	6-311++G**	cc-pVTZ
			Bond Lengths				
Zn1−N2	199.06	200.12	200.11	199.97	199.35	200.42	200.25
N2−C6	137.30	137.28	137.06	136.73	137.16	137.10	136.58
C6−C14	146.07	146.23	146.12	145.85	145.95	146.21	145.81
C6−N57	132.98	133.13	132.85	132.59	132.75	132.82	132.31
C14−C15	141.02	141.20	140.94	140.62	141.59	141.75	141.18
C14−C22	139.52	139.66	139.37	139.01	139.16	139.28	138.65
C22−C30	139.42	139.57	139.22	138.85	139.43	139.40	138.89
C30−C31	140.79	140.90	140.57	140.20	140.15	139.91	139.69
C22−X38	108.56	108.51	108.32	108.10	133.26	133.70	132.94
C30−X46	108.66	108.61	108.42	108.19	133.55	133.82	133.13
			Bond Angles				
Zn1N2C6	125.29	125.14	125.04	125.00	125.09	124.91	124.80
C6N2C7	109.41	109.72	109.92	110.00	109.83	110.18	110.40
N2C6C14	108.77	108.59	108.44	108.39	108.59	108.40	108.24
N2C6N57	127.53	127.44	127.50	127.44	127.79	127.69	127.65
C6C14C15	106.53	106.55	106.60	106.61	106.50	106.51	106.56
C15C14C22	121.08	121.06	121.02	121.00	120.62	120.48	120.53
C14C22C30	117.76	117.79	117.82	117.85	118.48	118.71	118.64
C22C30C31	121.16	121.15	121.15	121.14	120.90	120.82	120.83
C14C22X38	120.63	120.68	120.67	120.66	122.57	122.54	122.56
C22C30X46	119.60	119.61	119.63	119.64	120.15	120.23	120.19
C6N57C13	124.36	124.84	124.92	125.11	124.25	124.80	125.10

[a] Numbering is given in Figure 1. Distances in pm and angles in degrees.

The KCED25[50] least-squares fitting program was used to obtain the experimental parameters. The intensity and radial distribution curves are shown in Figures 2 and 4 for HPc-Zn and in Figures 3 and 5 for FPc-Zn.

Results and Discussion

Optimized Theoretical Geometry. The optimized geometry parameter values are given in Table 2. As can be seen, there are only small changes in the geometry for the different basis sets, which indicates that good predictions of the geometry may be obtained by the 6-31G* basis set compared to the far more time-consuming cc-pVTZ calculations. The agreement between the calculated geometry and the experimental derived geometry is very good, as can be seen in Tables 5 and 6. DFT force field calculations predict that both HPc-Zn and FPc-Zn have D_{4h} symmetry.

Comparison of the structural parameters for the different basis sets in Table 2 reveals small changes between HPc-Zn and FPc-Zn. The changes in bond lengths are usually less than 0.5 pm and smaller than 0.5° for bond angles. The only parameter that has a clear change is the bond angle C14−C22−X38, which increases by about 2° from HPc-Zn to FPc-Zn. This increase is probably due to the electrostatic repulsion between the electronegative atoms F38 and N57 bridge atom. This confirms the assumption that Pcs are little affected by peripheral substitution.

Molecular Vibrations and Flexibility. The MPcs have been commonly regarded as rigid molecules, but this is a rather doubtful description because of five vibrational frequencies (one degenerate) for HPc-Zn and ten vibrational frequencies (three degenerate) for FPc-Zn below 100 cm^{-1}. The lowest vibrational mode, B$_{2u}$, is 22 cm^{-1} for HPc-Zn and as low as 13 cm^{-1}for FPc-Zn. It is important to understand that the GED structure represents a molecular average structure which is the weighted (Boltzman) average over all vibrational states. Due to the low vibrational mode at 22 cm^{-1} (263 J mol^{-1}) and an experimental temperature of 750 K, which give $RT = 6240$ J mol^{-1} a large number of the vibrationally excited states are populated, and averaging over these states should give an average nonplanar molecular structure to be observed in GED if shrinkage is not included in the GED analysis. It is important to realize that the D_{4h} symmetry obtained by the DFT calculations (r_e structure) and a C_{4v} symmetry obtained by the GED method without shrinkage correction do not represent a serious disagreement. It simply represents two different molecular structures that are not directly comparable. Looking at the atomic displacements for the different vibrational modes for HPc-Zn shows that the atomic displacements of the Zn atom are small for the lowest mode except for the 124 cm^{-1} A$_{2u}$ mode, which shows a displacement of the Zn atom out of the symmetry plane. This mode has been simulated by calculating the potential energy as

TABLE 3: Experimental Parameters for HPc-Zn[a]

	rectilinear approach			curvilinear approch		
parameter	C_{4v}	D_{4h}	$D_{4h} + k_{h0}$	C_{4v}	D_{4h}	$D_{4h} + k_{h1}$
Zn1−N2	198.8(7)	197.8(6)	198.8(6)	198.8(7)	197.8(6)	198.9(6)
N2−C6	138.5(8)	137.0(5)	138.3(5)	138.4(8)	137.0(5)	138.2(5)
C6−N57	134.3(8)	132.8(5)	134.1(5)	134.2(8)	132.8(5)	134.0(5)
C6−C14	145.5(6)	145.2(6)	145.9(6)	145.6(6)	145.3(6)	146.0(6)
C14−C15	140.9(6)	141.9(4)	141.0(5)	140.9(6)	141.9(4)	141.2(5)
C14−C22	139.3(6)	140.3(4)	139.5(5)	139.4(6)	140.3(4)	139.4(5)
C22−C30	139.2(6)	140.2(4)	139.3(5)	139.2(6)	140.1(4)	139.5(5)
C30−C31	140.5(6)	141.5(4)	140.7(5)	140.6(6)	141.5(4)	140.7(5)
C22−H38	107.8(13)	106.7(12)	108.3(12)	107.9(12)	106.8(12)	108.6(12)
C30−H46	107.9(13)	106.8(12)	108.4(12)	108.0(12)	106.9(12)	108.7(12)
C7N2C6	107.6(9)	108.9(5)	107.6(7)	107.8(10)	108.9(5)	108.6(5)
C15C14C22	121.6(3)	122.0(2)	121.1(3)	121.6(3)	122.0(2)	121.1(3)
C14C22C30[b]	116.7(7)	115.9(5)	117.5(6)	116.7(7)	115.9(5)	117.7(8)
C22C30C31[b]	121.7(3)	122.1(2)	121.4(3)	121.7(3)	122.1(3)	121.2(4)
C14C22H38	120.6[c]	120.6[c]	120.6[c]	120.6[c]	120.6[c]	120.7[c]
C22C30H46	119.6[c]	119.6[c]	119.6[c]	119.6[c]	119.6[c]	119.6[c]
a1[d]	9.3(15)	0.0[c]	0.0	9.1(15)	0.0[c]	0.0[c]
a2[d]	73.8(49)	90.0[c]	90.0[c]	74.5(49)	90.0[c]	90.0[c]
a3[d]	98.0(68)	90.0[c]	90.0[c]	97.3(69)	90.0[c]	90.0[f]
a4[d]	96.7(53)	90.0[c]	90.0[c]	97.3(50)	90.0[c]	90.0[c]
N54A7A6[e]	75.3(46)	90.0[c]	90.0[c]	75.7(47)	90.0[c]	180.0[c]
h(Zn)[e]	32.3(51)	0.0	0.0	31.4(50)	0.0	0.0
R,[f] %	5.06	5.42	5.12	4.96	5.31	5.10

[a] r_a parameters. Parenthesized values are estimated error limits defined as $2.5(\sigma^2_{lsq} + (0.001r)^2)^{1/2}$, for distances and as $2.5\sigma_{lsq}$ for angles, where σ_{lsq} is one standard deviation taken from the least-squares refinements using a diagonal weight matrix and, the $0.001r$ term represents 0.1% uncertainty in the electron wavelength. The errors are in the units of the last digits. [b] Dependent parameter. [c] Fixed to their DFT calculated values. [d] See Figure 1 for definition. Zn1N2A1 = a1 (a1 is negative if the Zn atom is below the plane through the cavity N atoms), Zn1N2A2 = a2 + 90°, N2A1A3 = a3 + 90°, A1A2A3 = a4 + 90°. [e] The dihedral angle Zn1A6A7N54 is 0°, which gives the six-member ring consisting of the atoms Zn1, N2, C7, N54, C8, N3 a boat conformation. [f] $R = \{\sum_s w(I_s^{obs} - I_s^{calc})^2\}/\{\sum_s w(I_s^{obs})^2\} \times 100\%$, where w is a weight function usually equal to 1 and I is the molecular modified intensity.

TABLE 4: Experimental Parameters for FPc-Zn[a]

	rectilinear approach			curvilinear approch		
parameter	C_{4v}	D_{4h}	$D_{4h} + k_{h0}$	C_{4v}	D_{4h}	$D_{4h} + k_{h1}$
Zn1−N2	201.0(9)	199.6(8)	200.0(8)	200.8(8)	199.4(8)	200.0(8)
N2−C6	138.9(5)	137.8(5)	138.1(6)	139.0(5)	137.8(5)	138.1(5)
C6−N57	134.6(5)	133.5(5)	133.8(5)	134.6(5)	133.5(5)	133.8(5)
C6−C14	149.1(8)	145.3(10)	147.9(8)	149.1(8)	145.4(10)	147.9(8)
C14−C15	142.2(4)	142.6(4)	142.6(4)	142.2(4)	142.5(4)	142.6(4)
C14−C22	139.7(4)	140.0(4)	140.1(4)	139.7(4)	140.0(4)	140.1(4)
C22−C30	139.9(4)	140.2(4)	140.2(4)	139.8(4)	140.2(4)	140.2(4)
C30−C31	140.7(4)	141.0(4)	141.0(4)	140.7(4)	141.0(4)	141.0(4)
C22−F38	132.3(4)	132.5(5)	132.6(5)	132.3(4)	132.5(5)	132.6(5)
C30−F46	132.5(4)	132.7(5)	132.7(5)	132.5(4)	132.7(5)	132.7(5)
C7N2C6	105.8(12)	112.3(8)	111.2(7)	105.7(12)	112.1(7)	111.1(7)
C15C14C22	120.3(5)	120.5(4)	120.3(3)	120.5(5)	120.5(4)	120.5(3)
C14C22C30[b]	119.1(9)	118.7(8)	118.9(6)	118.7(9)	118.7(8)	118.8(6)
C22C30C31[b]	120.6(5)	120.8(4)	120.9(4)	120.8(5)	120.8(4)	120.8(4)
C14C22F38	121.2(9)	123.1(10)	123.4(7)	121.3(9)	123.1(8)	123.2(6)
C22C30F46	118.4(10)	119.4(12)	118.5(9)	118.5(11)	119.3(11)	118.5(9)
a1[d]	−2.3(30)	0.0[c]	0.0[c]	−1.9(25)	0.0[c]	0.0[c]
a2[d]	110.7(29)	90.0[c]	90.0[c]	164.2(28)	90.0[c]	90.0[c]
a3[d]	55.4(33)	90.0[c]	90.0[c]	54.5(32)	90.0[c]	90.0[c]
a4[d]	109.8(26)	90.0[c]	90.0[c]	109.6(26)	90.0[c]	90.0[c]
N54A7A6[e]	90.7(53)	90.0[c]	90.0[c]	91.0(51)	90.0[c]	90.0[c]
h(Zn)[e]	−7.9(86)	0.0	0.0	−6.7(81)	0.0	0.0
R,[f] %	4.55	6.06	4.84	4.31	5.85	4.57

[a] r_a parameters. Parenthesized values are estimated error limits defined as $2.5(\sigma^2_{lsq} + (0.001r)^2)^{1/2}$, for distances and as $2.5\sigma_{lsq}$ for angles, where σ_{lsq} is one standard deviation taken from the least-squares refinements using a diagonal weight matrix and, the $0.001r$ term represents 0.1% uncertainty in the electron wavelength. The errors are in the units of the last digits. [b] Dependent parameter. [c] Fixed to their DFT calculated values. [d] See Figure 1 for definition. Zn1N2A1 = a1 (a1 is negative if the Zn atom is below the plane through the cavity N atoms), Zn1N2A2 = a2 + 90°, N2A1A3 = a3 + 90°, A1A2A3 = a4 + 90°. [e] The dihedral angle Zn1A6A7N54 is 0°, which gives the six-member ring consisting of the atoms Zn1, N2, C7, N54, C8, N3 a boat conformation. [f] $R = \{\sum_s w(I_s^{obs} - I_s^{calc})^2\}/\{\sum_s w(I_s^{obs})^2\} \times 100\%$, where w is a weight function usually equal to 1 and I is the molecular modified intensity.

function of the distance, h, above the plane through the atoms N2 and N4 at the DFT/6-311++G** level. All structural parameters were optimized for fixed values of h. Starting with C_{4v} symmetry created serious convergence problems but reduc-

ing the symmetry to C_{2v} removed these problems. The potential energy function is shown in Figure 6. This clearly shows that the movement of the Zn atom out of the symmetry plane goes through C_{2v} symmetry and not C_{4v} symmetry. C_{2v} symmetry

TABLE 5: Comparison of the Structure Parameters for HPc-Zn[a]

parameter	GED, present work				cc-pVTZ	GED[8]			X-ray[13]
	$r_e{}^b$	u_{exp}	$u_{h1}{}^b$	$k_{h1}{}^b$	r_e	r	u	
				Bond Lengths					
Zn1−N2	198.2(6)	9.4(5)	8.2	0.169	199.1	195.4(29)[c]	5.1(44)	198.0
N2−C6	138.0(5)	5.9(2)	5.2	0.069	137.3	137.4(23)		136.9
C6−N57	133.6(5)[d]	5.5(2)	4.8	0.029	133.0			133.3
C6−C14	145.5(6)	6.1(2)	5.5	0.012	146.1	142.0(27)		145.5
C14−C15	140.7(5)	5.7(2)	5.0	0.003	141.0	155(10)		140.0
C14−C22	139.0(5)[d]	5.6(2)	4.9	−0.002	139.5	137.0(14)		139.3
C22−C30	138.9(5)[d]	5.6(2)	4.9	0.049	139.4	136.9		139.1
C30−C31	140.2(5)[d]	5.7(2)	5.0	0.003	140.8	139.9		139.6
C22−H38	106.9(12)	8.2(2)	7.6	0.073	108.6	112.2(82) av		
C30−H46	107.0(12)[d]	8.3(2)	7.6	0.077	108.7			
				Bond Angles					
C6N2C7	108.6(5)				109.4	106.9(46)		109.1
C15C14C22	121.1(3)				121.1	117.2(22)		121.3
C14C22C30	117.7(8)[e]				117.8	121.6		117.3
C22C30C31	121.2(4)[e]				121.2			121.4
C14C22H38	120.7[f]				120.7			
C22C30H46	119.6[f]				119.6			
R,[g] %	5.10					4.68		

[a] Parenthesized values are estimated error limits defined as $2.5(\sigma^2_{lsq} + (0.001r)^2)^{1/2}$, for distances and as $2.5\sigma_{lsq}$ for angles and amplitudes, where σ_{lsq} is one standard deviation taken from the least-squares refinements using a diagonal weight matrix and, the $0.001r$ term represents 0.1% uncertainty in the electron wavelength. The errors are in the units of the last digits. [b] Curvilinear treatment of the vibrating atoms (by SHRINK program). [c] Uncertainties are estimates of 2σ. [d] This value was calculated by using constraints between parameters (see text). [e] Dependent parameter. [f] This parameter was fixed at its B3LYP/cc-pVTZ calculated values. [g] $R = \{\sum_s w(I_s^{obs} - I_s^{calc})^2\}/\{\sum_s w(I_s^{obs})^2\} \times 100\%$, where w is a weight function usually equal to 1 and I is the molecular modified intensity.

TABLE 6: Calculated and Experimental Parameters of FPc-Zn[a]

parameter	GED, present work				cc-pVTZ
	$r_e{}^b$	u_{exp}	$u_{h1}{}^b$	$k_{h1}{}^b$	r_e
			Bond Length		
Zn1−N2	199.4(8)	10.0(7)	8.4	0.282	200.4
N2−C6	137.9(5)	5.3	5.3	0.097	136.9
C6−N57	133.2(6)[c]	4.8	4.8	−0.039	132.5
C6−C14	147.3(8)	5.6	5.6	−0.002	146.1
C14−C15	142.1(4)	5.2	5.2	−0.122	141.5
C14−C22	139.6(4)[c]	5.0	5.0	−0.041	139.0
C22−C30	139.9(4)[c]	5.0	5.0	0.091	139.1
C30-31C	141.7(4)[c]	5.0	5.0	0.103	139.9
C22−F38	131.8(5)	4.9	4.9	−0.079	133.2
C30−F46	132.0(5)[c]	4.9	4.9	−0.027	133.4
			Bond Angles		
C7N2C6	111.1(7)				110.4
C15C14C22	120.5(3)				120.5
C14C22C30	118.8(6)[d]				120.8
C22C30C31	121.4(4)[d]				120.9
C14C22F38	123.2(6)				122.6
C22C30F46	118.5(9)				120.2
R,[e] %	4.57[e]				

[a] Parenthesized values are estimated error limits defined as $2.5(\sigma^2_{lsq} + (0.001r)^2)^{1/2}$, for distances and as $2.5\sigma_{lsq}$ for angles and amplitudes, where σ_{lsq} is one standard deviation taken from the least-squares refinements using a diagonal weight matrix and, the $0.001r$ term represents 0.1% uncertainty in the electron wavelength. The errors are in the units of the last digits. [b] Curvilinear treatment of the vibrating atoms (by SHRINK program). [c] This value was calculated by using constraints between parameters (see text). [d] Dependent parameter. [e] $R = \{\sum_s w(I_s^{obs} - I_s^{calc})^2\}/\{\sum_s w(I_s^{obs})^2\} \times 100\%$, where w is a weight function usually equal to 1 and I is the molecular modified intensity.

allows two different N−Zn bond lengths and the splitting of these bond lengths, $\Delta r1 = r(N2−Zn) - 200.11$ and $\Delta r2 = r(N3−Zn) - 200.11$ are also shown in Figure 6. When the potential energy function is obtained the average height $\langle h \rangle = \int h \exp(-\Delta E/RT)\, dh \times [\int \exp(-\Delta E/RT)\, dh]^{-1}$ can be calculated.
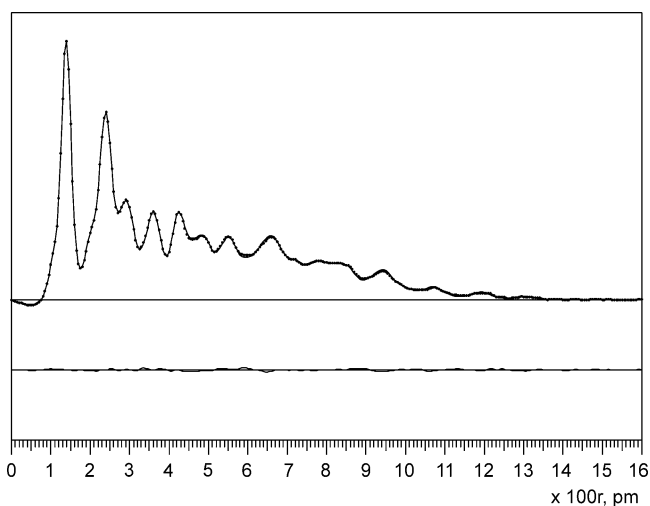

Figure 4. Radial distribution (RD) curves for HPc-Zn. The experimental points (dots) are the average of the four curves shown in Figure 2, and theoretical points are used for the unobserved region $s < 17.50$ nm^{-1}. The damping coefficient for the RD function is 35 pm^2. The curve below is the difference curve.

This gives $\langle h_{N2N3} \rangle = 14.5$ pm for the height from the Zn atom to the plane containing atoms N2 and N4, and correspondingly $\langle h_{N3N5} \rangle = 6.8$ pm. This explains the results obtained in the first GED investigation of HPc-Zn where $h = 34(13)$ pm.[7] However, it is not clear if shrinkage corrections have been applied in the second GED investigations of HPc-Zn.

Several IR and Raman investigations[12,14,51−59] on HPc-Zn have been made, and assignments of the vibrational frequencies have been discussed. Calculated frequencies at different level of theory have also been carried out and assignments to observed frequencies have been attempted.[12,56,57] Our high-level B3LYP/6-311++G** force field calculations together with calculated IR and Raman intensities give a good basis for assignments of the observed frequencies. A comparison of the observed vibrational frequencies from several different investigations have
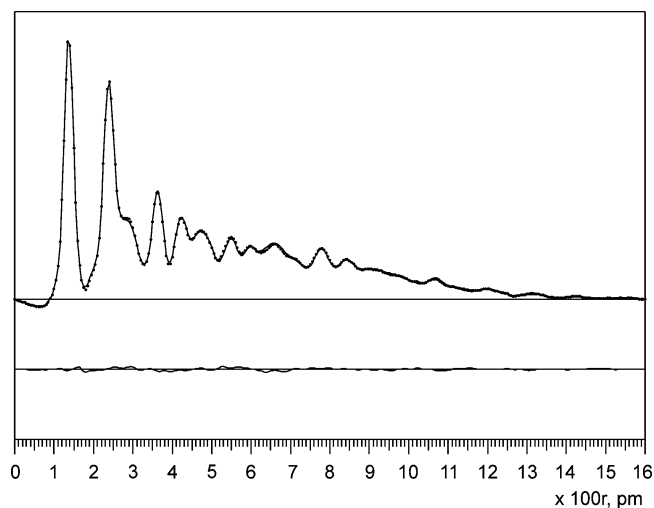
Molecular Structures of Phthalocyaninatozincs

J. Phys. Chem. A, Vol. 111, No. 47, 2007 **12017**

Figure 5. Radial distribution (RD) curves for FPc-Zn. The experimental points (dots) are the average of the four curves shown in Figure 3, and theoretical points are used for the unobserved region $s < 17.50$ nm^{-1}. The damping coefficient for the RD function is 35 pm^2. The curve below is the difference curve.
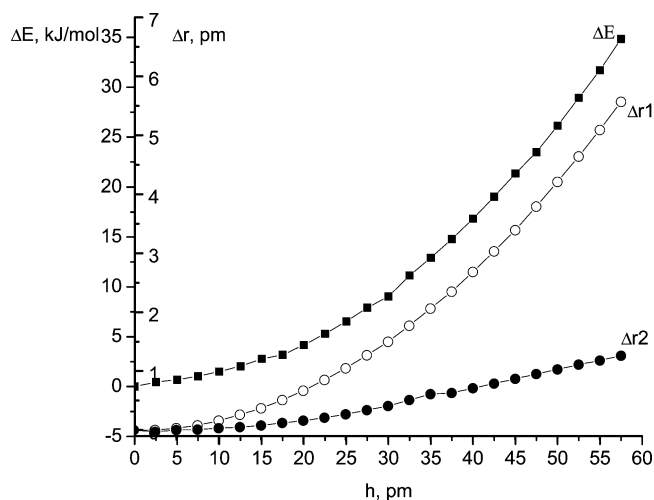

Figure 6. ΔE is the increase in energy as a function of the hight of the Zn atom, h, above the plane through the nitrogen atoms N2 and N4 as calculated by B3LYP/ 6-311++G**. For $h = 0.0$ pm the symmetry is D_{4h} and for all other values of h is the symmetry C_{2v}. $\Delta r1 = r(Zn1-N2) - r(Zn1-N2)_{h=0}$ and $\Delta r2 = r(Zn1-N3) - r(Zn1-N3)_{h=0}$. If the movement of the Zn atom had gone through C_{4v} symmetry $\Delta r1$ would be equal to $\Delta r2$.

been made and summarized in Table S3 and given as Supporting Information. The agreement between calculated and the proposed observed frequencies is very good. There is little information about vibrational frequencies for FPc-Zn; however, the B3LYP/6-311++G** calculated frequencies together with the calculated IR and Raman intensities should be a good basis for the assignment of the vibrational spectra for FPc-Zn.

Experimentally Derived Structure. As outlined above, it is important to understand the meaning of the determined structures and the importance of including the shrinkage effect particularly for planar molecules. The shrinkage effect can be included by using either a rectilinear approach (k_{h0}) or a curvilinear approach (k_{h1}). The r_a structure is transferred to a k_{h0} structure or a k_{h1} structure, which represents a geometrically consistent structure of averaged nuclear positions that is transferred back again to an r_a structure for a proper calculation of the molecular intensities. The r_e structure can be estimated from the r_a structure by using the $r_a - r_e$ correction term

calculated from the SHRINK program using the B3LYP/6-311G++G** force field. In Tables 3 and 4 are the experimental r_a structures given without correcting for shrinkage, correcting for shrinkage using k_{h0} values and k_{h1} values. As expected, the GED r_a structure without shrinkage correction gives a nonplanar structure. When shrinkage is included, the h parameter or angle $a1$ is approaching zero and start oscillating. Therefore D_{4h} symmetry was adopted in the final refinements. This strongly supports that the equilibrium structure has D_{4h} symmetry. It should be noted that the goodness-of-fit parameter, R, is slightly larger when shrinkage is included, compared to when shrinkage is not included. There might be two reasons for this, first that the C_{4v} model has more adjustable parameters, but more likely that the correction terms are based on the assumption that the atoms perform small amplitude motions about their equilibrium position, and this is probably not a very good approximation. However, the shrinkage corrected structure represents the best geometrical structure obtainable at the moment. It should also be noted that the very long C14-C15 bond length of 155(10) pm obtained in the previous GED investigations is not reproduced in our GED investigation. This is most likely due to the limited experimental data obtained for HPc-Zn.

It is of interest to compare the molecular structure of HPc-Zn and FPc-Zn, and in particular the changes in the benzo subunits. The C-C bond length in benzene[10] is 1.3975 pm and in hexafluorobenzene[60,61] 139.4(7) pm and 139.0 pm, a shortening of the C-C bond length is indicated. Perfluorination also causes shortening of the C=C bond length in ethylene.[62] A possible explanation for this effect is that the electronegative F atom draws electron density from the p-orbitals of the C atom, which leaves more s-character in the bonds between the C atoms. Because s-orbitals are more compact than p-orbitals the C-C bond lengths shortens.[61] The average C-C bond length calculated from B3LYP/cc-pVTZ given in Table 2 is 139.67 and 139.60 pm, respectively, for HPc-Zn and FPc-Zn. No overall shrinkage of the benzo subunits is predicted, where actually an increase is predicted for the C14-C15 bond length. However, comparing the experimental results indicates a small shortening of the bond length with 0.8 pm. This confirms both theoretically and experimentally that there are small changes in the molecular geometry with perfluorination of the benzo subunits. The only significant change is the increase of 2.5° for the C14-C22-X38 bond angle, which is expected due to the electrostatic repulsion between the electron negative N57 and F38 atoms.

Concluding Remarks. Our GED investigation is consistent with both HPc-Zn and FPc-Zn having D_{4h} equilibrium geometries as also is predicted by high-level quantum chemical calculations. There is a good agreement between the geometry obtained from the DFT calculations, our GED investigation, and the X-ray structure for HPc-Zn. There is also good agreement between the geometry obtained from the DFT calculations and our GED investigation for FPc-Zn. Calculated frequencies are valuable tools to assign the vibrational frequencies. It seems as the movement of the Zn atom out of the symmetry plane goes through C_{2v} symmetry and not C_{4v} symmetry. Both HPc-Zn and FPc-Zn are not rigid molecules but flexible molecules performing large movement about their equilibrium geometry. There are small structural differences between HPc-Zn and FPc-Zn; however, there are indications that the benzo subunits shrinks slightly when substituted with F atoms.

Supporting Information Available: Tables of Cartesian coordinates, frequencies, and IR and Raman intensities. This material is available free of charge via the Internet at http://pubs.acs.org.

References and Notes

(1) Kadish, K. M.; Smith, K. M.; Guilard R. *Application of Phthalocyanines*; The Porphyrin Handbook, Vol. 19; Academic Press: San Diego, CA, 2003.

(2) Kadish, K. M.; Smith, K. M.; Guilard, R. *Phthalocyanines: Properties and Materials*; The Porphyrin Handbook, Vol. 17; Academic Press: San Diego, CA, 2003.

(3) Kadish, K. M.; Smith, K. M.; Guilard, R. *Phthalocyanines: Spectroscopic and Electrochemical Characterization*; The Porphyrin Handbook, Vol. 16; Academic Press: San Diego, CA, 2003.

(4) Engel, M. K. *Single-crystal structures of phthalocyanine complexes and related macrocycles*; The Porphyrin Handbook, Vol. 20; Academic Press: San Diego, CA, 2003.

(5) McKeown, N. B. *Phthalocyanine Materials: Structure, Synthesis and Function*; Cambridge University Press: Cambridge, U.K., 1998.

(6) Leznoff, C. C.; Lever, A. B. P. *Phthalocyanines - Properties and Applications*; VCH Publishers: New York; Vol. 1 (1989), Vol. 2 (1992), Vol. 3 (1993). Vol. 4 (1996).

(7) Mihill, A.; Buell, W.; Fink, M. *J. Chem. Phys.* **1993**, *99*, 6416.

(8) Ruan, C.-y.; Mastryukov, V.; Fink, M. *J. Chem. Phys.* **1999**, *111*, 3035.

(9) Mastryukov, V.; Ruan, C. y.; Fink, M.; Wang, Z.; Pachter, R. *J. Mol. Struct.* **2000**, *556*, 225.

(10) Gundersen, S.; Samdal, S.; Strand, T. G.; Volden, H. V. *J. Mol. Struct.* **2007**, *832*, 164.

(11) Samdal, S.; Volden, H. V.; Ferro, V. R.; Garcia de la Vega, J. M.; Gonzalez-Rodriguez, D.; Torres, T. *J. Chem. Phys.* **2007**, *111*, 4542.

(12) Tackley, D. R.; Dent, G.; Smith, W. E. *Phys. Chem. Chem. Phys.* **2000**, *2*, 3949.

(13) Scheidt, W. R.; Dow, W. *J. Am. Chem. Soc.* **1977**, *99*, 1101.

(14) Tackley, D. R.; Dent, G.; Smith, W. E. *Phys. Chem. Chem. Phys.* **2001**, *3*, 1419.

(15) Porezag, D.; Pederson, M. R. *Phys. Rev. B* **1996**, *54*, 7830.

(16) Halls, M. D.; Schlegel, H. B. *J. Chem. Phys.* **1998**, *109*, 10587.

(17) Johnson, B. G.; Florian, J. *Chem. Phys. Lett.* **1995**, *247*, 120.

(18) Halls, M. D.; Schlegel, H. B. *J. Chem. Phys.* **1999**, *111*, 8819.

(19) Zeil, W.; Haase, J.; Wegmann, L. *Z. Instrumentenkunde* **1966**, *74*, 84.

(20) Martinsen, K.-G., Volden, H. V. *Annual Report 1993 from the Norwegian GED-Group.* 1993.

(21) Martinsen, K.-G. Dissertations submitted to the Faculty of Matematics and Natural Sciences, University of Oslo, 1997.

(22) Gundersen, S.; Samdal, S.; Seip, R.; Strand, T. G. *J. Mol. Struct.* **2004**, *691*, 149.

(23) Ross, A. W.; Fink, M.; Hilderbrandt, R. *International Tables for Crystallography*; Kluwer Academic Publishers: Dordrecht, The Netherlands, 1992.

(24) Gundersen, G., Samdal, S. *Annual Report 1976 from the Norwegian GED-Group.* 1976.

(25) Frisch, M. J.; Trucks, G. W.; Schlegel, H. B.; Scuseria, G. E.; Robb, M. A.; Cheeseman, J. R.; Montgomery, J. A., Jr.; Vreven, T.; Kudin, K. N.; Burant, J. C.; Millam, J. M.; Iyengar, S. S.; Tomasi, J.; Barone, V.; Mennucci, B.; Cossi, M.; Scalmani, G.; Rega, N.; Petersson, G. A.; Nakatsuji, H.; Hada, M.; Ehara, M.; Toyota, K.; Fukuda, R.; Hasegawa, J.; Ishida, M.; Nakajima, T.; Honda, Y.; Kitao, O.; Nakai, H.; Klene, M.; Li, X.; Knox, J. E.; Hratchian, H. P.; Cross, J. B.; Adamo, C.; Jaramillo, J.; Gomperts, R.; Stratmann, R. E.; Yazyev, O.; Austin, A. J.; Cammi, R.; Pomelli, C.; Ochterski, J. W.; Ayala, P. Y.; Morokuma, K.; Voth, G. A.; Salvador, P.; Dannenberg, J. J.; Zakrzewski, V. G.; Dapprich, S.; Daniels, A. D.; Strain, M. C.; Farkas, O.; Malick, D. K.; Rabuck, A. D.; Raghavachari, K.; Foresman, J. B.; Ortiz, J. V.; Cui, Q.; Baboul, A. G.; Clifford, S.; Cioslowski, J.; Stefanov, B. B.; Liu, G.; Liashenko, A.; Piskorz, P.; Komaromi, I.; Martin, R. L.; Fox, D. J.; Keith, T.; Al-Laham, M. A.; Peng, C. Y.; Nanayakkara, A.; Challacombe, M.; Gill, P. M. W.; Johnson, B.; Chen, W.; Wong, M. W.; Gonzalez, C.; Pople, J. A. *Gaussian 03*, revision B.03; Gaussian, Inc.: Pittsburgh, PA, 2003.

(26) Becke, A. D. *J. Chem. Phys.* **1993**, *98*, 5648.

(27) Lee, C.; Yang, W.; Parr, R. G. *Phys. Rev. B* **1988**, *37*, 785.

(28) Ferro, V. R.; Poveda, L. A.; Claessens, C. G.; Gonzalez-Jonte, R. H.; Garcia de la Vega, J. M. *Int. J. Quantum Chem.* **2003**, *91*, 369.

(29) Gong, X. D.; Xiao, H. M.; Gao, P.; Tian, H. *THEOCHEM* **2002**, *587*, 189.

(30) Ferro, V. R.; Garcia de la Vega, J. M.; Claessens, C. G.; Poveda, L. A.; Gonzalez-Jonte, R. H. *J. Porphyrins Phthalocyanines* **2001**, *5*, 491.

(31) Ferro, V. R.; Garcia de la Vega, J. M.; Gonzalez-Jonte, R. H.; Poveda, L. A. *THEOCHEM* **2001**, *537*, 223.

(32) Ryeng, H.; Ghosh, A. *J. Am. Chem. Soc.* **2002**, *124*, 8099.

(33) Vangberg, T.; Lie, R.; Ghosh, A. *J. Am. Chem. Soc.* **2002**, *124*, 8122.

(34) Wasbotten, I. H.; Wondimagegn, T.; Ghosh, A. *J. Am. Chem. Soc.* **2002**, *124*, 8104.

(35) Ghosh, A. *J. Porphyrins Phthalocyanines* **2000**, *4*, 380.

(36) Nguyen, K. A.; Pachter, R. *J. Phys. Chem A* **2000**, *104*, 4549.

(37) Parusel, A. B. J.; Ghosh, A. *J. Phys. Chem. A* **2000**, *104*, 2504.

(38) Parusel, A. B. J.; Wondimagegn, T.; Ghosh, A. *J. Am. Chem. Soc.* **2000**, *122*, 6371.

(39) Hariharan, P. C.; Pople, J. A. *Mol. Phys.* **1974**, *27*, 209.

(40) Krishnan, R.; Binkley, J. S.; Seeger, R.; Pople, J. A. *J. Chem. Phys.* **1980**, *72*, 650.

(41) Frisch, M. J.; Pople, J. A.; Binkley, J. S. *J. Chem. Phys.* **1984**, *80*, 3265.

(42) Dunning, T. H., Jr. *J.Chem. Phys.* **1989**, *90*, 1007.

(43) Balabanov, N. B.; Peterson, K. A. *J. Chem. Phys.* **2005**, *123*, 064107/1.

(44) Seip, H. M. *Specialist Periodical Reports: Molecular Structure by Diffraction Methods*; Sim, G. A., Sutton, L. E., Eds.; The Chemical Society, London, 1973; Vol. 1, p 7.

(45) Hargittai, I., Hargittai, M., Eds. Stereochemical Applications of Gas-Phase Electron Diffraction, Pt. A: The Electron Diffraction Technique. *Methods Stereochem. Anal.* **1988**, *10*, 1988.

(46) Hedberg, L.; Mills, I. M. *J. Mol. Spectrosc.* **1993**, *160*, 117.

(47) Hedberg, L.; Mills, I. M. *J. Mol. Spectrosc.* **2000**, *203*, 82.

(48) Sipachev, V. A. *THEOCHEM* **1985**, *22*, 143.

(49) Sipachev, V. A. *J. Mol. Struct.* **2001**, *567−568*, 67.

(50) Gundersen, G.; Samdal, S.; Seip, H.-M.; Strand, T. G. Annual Report 1977, 1980, 1981 from the Norwegian Gas Electron Diffraction Group.

(51) Kobayashi, T. *Spectrochim. Acta* **1970**, *26*, 1313.

(52) Kobayashi, T.; Kurokawa, F.; Uyeda, N.; Suito, E. *Spectrochim. Acta* **1970**, *26*, 1305.

(53) Terzian, G.; Moubaraki, B.; Mossoyan-Deneux, M.; Benlian, D. *Spectrochim. Acta.* **1989**, *45A*, 675.

(54) Aroca, R.; Zeng, Z. Q.; Mink, J. *J. Phys. Chem. Solids* **1990**, *51*, 135.

(55) Gobernado-Mitre, I.; Aroca, R.; DeSaja, J. A. *Spectrochim. Acta* **1994**, *50A*, 1243.

(56) Ding, H.; Wang, S.; Xi, S. *J. Mol. Struct.* **1999**, *475*, 175.

(57) Gladkov, L. L.; Shkirman, S. F.; Sushko, N. I.; Konstantinova, V. K.; Sokolov, N. A.; Solovyov, K. N. *Spectrosc. Lett.* **2001**, *34*, 709.

(58) Seoudi, R.; El-Bahy, G. S.; El Sayed, Z. A. *J. Mol. Struct.* **2005**, *753*, 119.

(59) Szybowicz, M.; Runka, T.; Drozdowski, M.; Bala, W.; Wojdyla, M.; Grodzicki, A.; Piszczek, P.; Bratkowski, A. *J. Mol. Struct.* **2007**, *830*, 14.

(60) Almenningen, A.; Bastiansen, O.; Seip, R.; Seip, H. M. *Acta Chem. Scand.* **1964**, *18*, 2115.

(61) Braden, D. A.; Hudson, B. S. *J. Phys. Chem. A* **2000**, *104*, 982.

(62) Carlos, J. L., Jr.; Karl, R. R., Jr.; Bauer, S. H. *J. Chem. Soc., Faraday Trans. 2* **1974**, *70*, 177.